Disproportionation of [(py)(NH 3) 4 Ru III] at the N7 of Guanine Nucleosides: Severing the N - Glycosidic Bond

ARTICLE *in* INORGANIC CHEMISTRY · OCTOBER 1996

Impact Factor: 4.76 · DOI: 10.1021/ic960798g

3 AUTHORS, INCLUDING:

Michael J Clarke
Boston College, USA
84 PUBLICATIONS **3,039** CITATIONS

SEE PROFILE

Disproportionation of [(py)$(NH_3)_4Ru^{III}$] at the N7 of Guanine Nucleosides: Severing the *N*-Glycosidic Bond

K. J. LaChance-Galang,† M. Zhao, and M. J. Clarke*

Merkert Chemistry Center, Boston College, Chestnut Hill, Massachusetts 02167

Received July 10, 1996[⊗]

Under optimal conditions, the N7-coordinated complexes *trans*-[L(py)$(NH_3)_4Ru^{III}$] (L = Guo, dGuo, 1MeGuo) disproportionate to give ∼50% *trans*-[Guo(py)$(NH_3)_4Ru^{II}$] and a putative Ru^{IV} species that yields ∼50% [Gua(py)$(NH_3)_4Ru^{III}$]. Disproportionation follows the rate law $d[Ru^{II}]/dt = k_o[Ru^{III}] + k_1[OH^-][Ru^{III}]$ (for L = Guo: $k_o = 2.9 \times 10^{-4}$ s^{-1}, $k_1 = 6.4$ M^{-1} s^{-1}) so that the rate-limiting step in the dominant, hydroxide-dependent pathway is not electron transfer between Ru^{III}'s, but probably deprotonation of an ammine. Consistent with the ordering of k_1's for the ligands (1MeGuo > Guo ∼ dGuo > 9MeGua ≫ Gua), ionization of the purine at N1 or N9 slows the disproportionation by suppressing ammine ionization. Activation parameters for k_1 (pH = 11.50) with L = Guo are as follows: $\Delta H^{\ddagger} = 17.4 \pm 0.8$ kcal/mol ($E_a = 18.0 \pm 0.8$ kcal/mol), and $\Delta S^{\ddagger} = 2.4 \pm 0.1$ cal/(mol K). Following disproportionation, the appearance of *trans*-[Gua(py)$(NH_3)_4Ru^{III}$] and free ribose is consistent with general acid hydrolysis of the glycosidic bond induced by Ru^{IV}, which is subsequently reduced. The rate of appearance of *trans*-[Gua(py)$(NH_3)_4Ru^{III}$] (pH 9.2−11.9) is complicated by purine loss, anation and possibly redox reactions, so that a net hydroxide dependence of approximately $[OH^-]^{1/2}$ was observed. Activation parameters for k_{obs} (pH 11.90) with L = Guo are as follows: $\Delta H^{\ddagger} = 24.6 \pm 1.6$ kcal/mol ($E_a = 25.2 \pm 1.6$ kcal/mol), $\Delta S^{\ddagger} = 8.9 \pm 0.8$ cal/(mol K). In the presence of oxygen, *trans*-[8-OGuo(py)$(NH_3)_4Ru^{III}$] was detected as a minor product, but neither 8-oxoguanine nor complexes involving it were observed.

Introduction

The presence of $(NH_3)_5Ru^{III}$ at the N7 of purine nucleosides has long been known to lead to cleavage of the *N*-glycosidic bond of Guo and dGuo by a general acid route.[1] Ruthenium(III) also assists autoxidation to 8-oxonucleosides, in which the *N*-glycosidic bond should be susceptible to base hydrolysis.[2,3] Such scission of the glycosidic bond often leads to DNA strand cleavage; however, neither of these reactions is efficient at cleaving DNA.[4] One way of improving the metal as a general acid is to increase its charge by raising its oxidation state. However, since metal ions in the IV or higher oxidation states require strong acid to prevent hydrolysis to oxo-species, it is difficult to prepare such complexes with DNA or its constituent bases. One approach is to coordinate the metal ion in a lower oxidation state and then oxidize it to M^{IV} *in situ*, but most reagents of sufficient oxidizing power would also damage the DNA.

Complexes such as [py$(NH_3)_5Ru^{III}$] spontaneously disproportionate at neutral pH to form the corresponding Ru^{II} and Ru^{IV} species following an approximate second-order rate law,[5] thereby providing a convenient route to Ru^{IV} without the addition of an oxidant. We now report the first efficient hydrolytic mechanism for cleaving the *N*-glycosidic bond by a metal ion serving as a general acid catalyst at G[7]. The reaction appears to be analogous to the *N*-glycosidic bond scission step in the Maxam−Gilbert reaction for sequencing at guanine residues.[6,7]

Abbreviations. Guo, guanosine; 1MeGuo, 1-methylguanosine; Gua, guanine; 9MeGua, 9-methylguanine; dG, 2′-deoxyguanosine; 8-OGuo, 8-oxoguanosine; 1Me8-OGuo, 1-methyl-8-oxoguanosine; G[7], N7 of guanine; Ino, inosine; Isn, isonicotinamide; RuGua, *trans*-[Gua(py)$(NH_3)_4Ru^{III}$]; RuGuo, *trans*-[Guo(py)$(NH_3)_4Ru^{III}$].

Experimental Section

Materials. $RuCl_3$ (Johnson Matthey), guanosine (Aldrich), 1-methylguanosine (Sigma), 9-methylguanine, and 2′-deoxyguanosine (Fluka) were used without further purification. *trans*-[(SO_4)(py)$(NH_3)_4$Ru]Cl was prepared by the method of Isied.[8]

***trans*-[(Guo)(py)$(NH_3)_4$Ru]Cl_3.** A 100 mg sample of *trans*-[(py)-$(SO_4)(NH_3)_4$Ru]Cl was dissolved in a minimum volume (∼5 mL) of water and reduced with zinc amalgam for 20 min under argon. A 2:1 molar ratio of guanosine was introduced into the red solution and the reduction was allowed to continue for 3 h resulting in a yellow-orange solution. The zinc amalgam and the undissolved ligand were removed by filtration with two washings. The combined filtrate (15 mL) was acidified with 3 M HCl and 30% H_2O_2 was added dropwise with stirring at intervals of 5 min until a royal blue solution was obtained. Acetone (100−150 mL) was added to induce precipitation. After the mixture was cooled for 0.5 h, the solid was collected by filtration, redissolved, and loaded onto a SP-Sephadex C-25 ion exchange column (10 cm × 1.8 cm). The band of interest was eluted with 0.3 M HCl. The volume of the band was reduced to a minimum by rotary evaporation and acetone was added to induce precipitation. Occasionally a turquoise band containing *trans*-[(8O-Guo)(py)$(NH_3)_4$Ru]Cl_2 was eluted with 0.2 M HCl (see 1Me8O-Guo below). Anal. Calcd for [Ru$(NH_3)_4$-(py)(Guo)]Cl_3·2.5H_2O: C, 26.38; H, 5.18; N, 20.51; Cl, 15.57. Found: C, 26.51; H, 4.81; N, 20.34; Cl, 15.64. UV−vis (λ_{max} nm (ϵ M^{-1} cm^{-1})): 251 (19 700), 277 (sh) (12 700), 328 (2280), 621 (680).

† Present Address: Regis College, Weston, MA.

⊗ Abstract published in *Advance ACS Abstracts,* September 15, 1996.

(1) Clarke, M. J.; Morrissey, P. E. *Inorg. Chim. Acta* **1984**, *80*, L69−70.
(2) Gariepy, K. C.; Curtin, M. A.; Clarke, M. J. *J. Am. Chem. Soc.* **1989**, *111*, 4947−52.
(3) Kasprzak, K. S.; Hernandez, L. *Cancer Res.* **1989**, *49*, 5964−68.
(4) Clarke, M. J.; Jansen, B.; Marx, K. A.; Kruger, R. *Inorg. Chim. Acta* **1986**, *124*, 13−28.
(5) Rudd, D. P.; Taube, H. *Inorg. Chem.* **1971**, *10*, 1543−1544.
(6) Maxam, A. M.; Gilbert, W. *Methods Enzymol.* **1980**, *65, Part 1*, 499−560.
(7) Maxam, A. M.; Gilbert, W. *Proc. Natl. Acad. Sci. (U.S.A.)* **1977**, *110*, 119.
(8) Isied, S.; Taube, H. *Inorg. Chem.* **1976**, *15*, 3070−3075.

S0020-1669(96)00798-7 CCC: $12.00

^{1}H NMR (δ ppm): Ru^{III}Guo, H8, −28.2; H1′, 13.8; H2′, 2.7; H3′, 4.7; H4′, 5.1; H5′, 5.2; py, H2, −10.7; H3, 9.6; H4, −22.5; Ru^{II}Guo, H8, 8.05 s; H1′, 5.85 d; H2′, hidden by HOD; H3′, 3.75 m; H4′, 4.14 d; H5′, 4.32 t; py, H2, 8.46 d; H3, 7.28 t; H4, 7.67 t; $Ru^{II}Guo^-$, H8, 7.85 s; H1′, 5.64 d; H2′, hidden by HOD; H3′, 3.75 q; H4′, 4.11 d; H5′, obscured by HOD; py, H2, 8.45 d; H3, 7.24 t; H4, 7.62 t. $E°$(pH 1) = 401 mV vs NHE. Ionization constants determined from Pourbaix plots fit to the equation $E_h = E° - 0.59 \log([H^+] + K_a(Ru^{II})/[H^+] + K_a(Ru^{III}))$ are $pK_a(Ru^{III}) = 7.9 \pm 0.1$ and $pK_a(Ru^{II}) = 10.3 \pm 0.1$. *trans*-$[(Guo)(py)(NH_3)_4Ru^{II}]$ was prepared in situ by reduction of *trans*-$[(Guo)(py)(NH_3)_4Ru]Cl_3$ over zinc amalgam under an argon atmosphere.

***trans*-[(dGuo)(py)$(NH_3)_4$Ru]Cl_3** was similarly synthesized; however, it could not be subjected to ion-exchange chromatography as acid eluants hydrolyzed the *N*-glycosidic bond while neutral ones induced disproportionation of the metal ion. Consequently, the complex was isolated by reducing the volume after oxidation and then precipitating with acetone. ^{1}H NMR and HPLC showed these samples to contain variable amounts (10−50%) of $[(Gua)(py)(NH_3)_4Ru]$ as the sole contaminant. UV−vis (λ_{max} nm): 254, 275 (sh), 330, 623. ^{1}H NMR (δ ppm): Guo: H8, −28.0; H1′, 13.0; H2′ - H5′, 1.2 - 5.6; py, H2, −10.5; H3, 9.6; H4, −22.5. $E° = 461$ mV. Ionization constants determined from Pourbaix plots are as follows: $pK_a(Ru^{III}) = 8.24 \pm 0.17$ and $pK_a(Ru^{II}) = 9.65 \pm 0.18$.

***trans*-[(1MeGuo)(py)$(NH_3)_4$Ru]Cl_3** was synthesized in a manner similar to *trans*-$[(Guo)(py)(NH_3)_4Ru]Cl_3$. Anal. Calcd for $[(1MeGuo)(py)(NH_3)_4Ru]Cl_3 \cdot 4H_2O$: C, 26.54; H, 5.58; N, 19.35; Cl, 14.69. Found: C, 26.66; H, 4.98; N, 19.22; Cl, 14.51. UV−vis (λ_{max} nm (ϵ M^{-1} cm^{-1})): 253 (19 600), 277 (sh) (13 700), 319 (2280), 633 (930). ^{1}H NMR (δ ppm): 1MeGuo, H8, −28.5; CH_3(1), 6.7; H1′, 14.5; H2′, 2.8; H3′, 4.8; H4′, 5.2; H5′, 5.3; py, H2, −11.0; H3, 9.9; H4, −23.1. $E° = 393$ mV vs NHE.

***trans*-[(9MeGua)(py)$(NH_3)_4$Ru]Cl_3** was synthesized in a manner similar to *trans*-$[(Guo)(py)(NH_3)_4Ru]Cl_3$. Anal. Calcd for $[Ru(NH_3)_4(py)(9\text{-}MeGua)]Cl_3 \cdot 3H_2O$: C, 23.02; H, 5.28; N, 24.41; Cl, 18.53. Found: C, 23.28; H, 4.76; N, 24.01; Cl, 18.88. UV−vis (λ_{max} nm (ϵ M^{-1} cm^{-1})): 249 (16 400), 275 (sh) (9940), 340 (2290) 624 (699); 9MeGua$^-$, 246, 339, 710. ^{1}H NMR (δ ppm): 9MeGua, H8, −30.8; CH_3(9), 20.3; py, H2, −11.1; H3, 11.6; H4, −24.8. $E° = 397$ mV vs NHE.

***trans*-[(Gua)(py)$(NH_3)_4$Ru]Cl_3** was prepared by hydrolyzing *trans*-$[(dGuo)(py)(NH_3)_4Ru]Cl_3$ in acid for several hours. The resulting royal blue complex was then purified on an SP-Sephadex column with the desired band eluting with 0.3 M HCl. This fraction was rotary evaporated to a small volume and acetone added to induce precipitation. A blue powder was obtained upon filtration. Anal. Calcd for $[(Gua)(py)Ru(NH_3)_4]Cl_3 \cdot 2.5H_2O$ C, 21.80; H, 4.95; N, 25.43; Cl, 19.31. Found: C, 22.36; H, 4.48; N, 25.21; Cl, 19.18. UV−vis (λ_{max} nm (ϵ M^{-1} cm^{-1})): 246 (16 800), 274 (sh) (9980), 317 (2260) 622 (629). ^{1}H NMR (δ ppm): Gua, H8, −34.0; py, H2, −11.5; H3, 11.5; H4, −24.5; Gua^{2-}, H8, −70.1; py, H2, −17.2; H3, 20.8; H4, −31.1. $[(Gua^{2-})(py)Ru(NH_3)_4]$, pH = 12, UV−vis ($\lambda_{max}$ nm (ϵ M^{-1} cm^{-1})): 788 (∼2100). $E°$(pH 1−2) = 369 mV. pK_{a1}(N9) = 4.92 ± 0.02, pK_{a2} (N1) = 10.0 ± 0.2.

***trans*-[(1Me8-OGuo)(py)$(NH_3)_4$Ru]Cl_2** was prepared by allowing a solution of *trans*-$[(1MeGuo)(py)(NH_3)_4Ru]Cl_3$ at pH 8 to stand for several hours. The pH of the solution was then lowered to ∼2 before oxidation with H_2O_2, Ce^{4+}, or air. The oxidized solution was chromatographed on an SP-Sephadex column from which the turquoise band eluted with 0.2 M HCl. Yield: 6%. Anal. Calcd for $[Ru(NH_3)_4(py)(1Me8\text{-}OGuo)]Cl_3 \cdot HCl$: C, 28.77; H, 4.84; N, 20.97. Found: C, 28.85; H, 4.73; N, 21.05. UV−vis (λ_{max} nm (ϵ M^{-1} cm^{-1})): 251 (11 300), 289 (10 600), 350 (sh) (2310), 776 (4140). ^{1}H NMR (δ ppm): 1-Me-8-OGuo, CH_3(1), −2.6; H1′−H5′, 3−7; py, H2, −23.0; H3, 21.0; H4, −31.6. $E°$(pH 5.5) = −7 mV.

Instrumentation. NMR spectra were obtained on a Varian Unity 300 MHz FT NMR spectrometer. Water in the samples was removed by three successive dissolutions in D_2O followed by lyophilization. A typical sample was prepared by dissolving 10 mg of the compound in 0.5−0.7 mL of D_2O, which was then transferred into a 5 mm NMR tube. pH (uncorrected for the isotope effect) was adjusted using dilute solutions of NaOD and DCl. UV−vis spectra were run on a Cary 2400 spectrophotometer. Elemental analyses were done by Robertson Microlit Laboratories Inc.

Reduction potentials on couples, which were determined to be reversible by cyclic voltammetry, were measured on 1−2 mM solutions in 0.1 M LiCl as the position of the square wave voltammetry peak generated by a BAS Model 100A potentiostat. The working electrode was carbon paste, the reference electrode was Ag/AgCl, and the counter electrode was platinum wire. Potentials are reported relative to the NHE by using $[(NH_3)_6Ru^{III/II}]$ (57 mV vs NHE) as an internal reference.

GC/MS was done on a Hewlett-Packard 5980 II gas chromatograph interfaced with a HP 5972 mass spectrometer with a split injection flow rate of 45 mL/min. Capilliary columns were 30 m coated with HP-5MS (programmed from 100 to 280 °C at 5 °C/min and held at the final temperature for 15 min) or J&W DB-17 (held at 80 °C for 2 min and then ramped at 10 °C/min to 285 °C, where it was held for 25 min).

Kinetic Measurements. Redox reactions were run in phosphate buffer with the ionic strength adjusted to 0.1 M with NaCl. The pH of the solution was measured with a Cole-Parmer combination pH electrode connected to an Orion model SA520 pH meter. Temperatures were adjusted using a Haake D3 thermostat and a Haake G water bath. The disproportionation reaction was monitored as a function of pH by following the increase in absorbance at 412 or 415 nm, depending on the complex. The data was then fitted to a first-order kinetics expression.

The hydrolysis reaction was monitored as a function of pH by following the increase in the $[(Gua^{-,2-})py(NH_3)_4Ru^{III}]$ LMCT band under an argon atmosphere, so that there would be no interference from the autoxidation reaction. In order to minimize overlap between the $Gua^{1-,2-} \rightarrow Ru^{III}$ LMCT absorbance and those from (1) the deprotonated Guo complex, (2) MLCT bands arising from the disproportionation of the Gua complex, and (3) possible bands due to ammine loss through SN_1CB anation reactions, the rate of appearance of $[(Gua^-)py(NH_3)_4Ru^{III}]$ was followed by the increase in absorbance at the λ_{max} for the LMCT band (700−790 nm, depending on the protonation state of the complex at a given pH). Absorbance vs time data was fitted to the equation: $A = A_\infty(1 - e^{-kt})$, where A is the absorbance at a given time and A_∞ is the maximum absorbance. Estimates of k_{obs} by this method agreed reasonably well with those derived from fits to the sequential rate equation.[9]

Analysis of Hydrolysis Products. Products from the reactions of *trans*-$[Guo(py)(NH_3)_4Ru^{III}]$ at high pH were analyzed by ^{1}H NMR and ion-exchange chromatography. Quantification of $[Guo(py)(NH_3)_4Ru^{II}]$ was made from its absorbance at 415 nm. Following the reaction, the pH was adjusted to 1−2 and the solution was oxidized with one of the following oxidants—(1) 50/50 3 M HCl/30% H_2O_2, (2) acidic Ce^{IV}, or (3) air—until the solution reverted to its original royal blue color. Anionic and neutral organic materials were separated from the hydrolysis reaction mixture by elution with water from an SP-Sephadex column, which retained the metal complexes. The water fraction was rotary evaporated to dryness and a portion of the salt eliminated by dissolving the residue in absolute ethanol and filtering. The filtrate containing ribose and other organics was then evaporated to dryness. Since Sephadex degrades to dextrose in acid, the organic samples are tainted with varying amounts of this hexose. Thin layer chromatography to detect ribose was performed on silica gel coated on aluminum plates with absolute methanol as the mobile phase. The spots were made visible by charring with a heat gun. Small portions (∼1 mL) of the organic fractions were mixed with 4 mL of Bial's reagent (orcinol in concentrated HCl containing a trace of ferric chloride catalyst, which produces a green color in the presence of aldopentoses)[10] and placed in a boiling water bath for one minute. A test for base propenal with 2-thiobarbituric acid was negative.[10] A hydrolysis reaction was performed in the dark to prevent the possibility of photopolymerization of a possible sugar oxidation product, 5-methylene-2-furanone.[11,12] After this solution was neutralized with acid and extracted with chloroform,

(9) Moore, J. W.; Pearson, R. G. *Kinetics and Mechanism*; Wiley: New York, 1981; pp 290−300.
(10) Armstrong, R.; Baechler, R.; Dulak, L.; Glaros, G.; Klappmeier, F. *Laboratory Chemistry A Life Science Approach*; Macmillan Publishing Co., Inc.: New York, 1980, pp 272−273.
(11) Thorp, H. H. *Met. Ions Biol. Syst.* **1996**, *33*, 297−324.

HPLC scans gave no evidence of 5-methylene-2-furanone.[11,12] Reactant mixtures of [Guo$(NH_3)_4$(py)Ru^{III}] were also subjected to GC/MS analysis. After allowing these to react in air at room temperature for 2 h at pH 10.5, solutions were rotary evaporated to dryness and treated with BSTFA/pyridine at 85 °C for 30 min and then analyzed by GC/MS. These analyses revealed ribose and related isomers, guanine, and small amounts of 8-oxoguanine, but no 5-methylene-2-furanone.

Several colored bands containing various ruthenium complexes were eluted from SP-Sephadex with increasing concentrations of HCl. These bands were reduced to a minimum volume by rotary evaporation, followed by addition of acetone to precipitate the complex, which was collected by filtration. The relative amounts of the [L(py)$(NH_3)_4Ru^{III}$] (L = Guo, Gua and 8-OGuo) were assayed by condensing the band in which these eluted, followed by quantitatively precipitating the complexes with acetone. Samples were then prepared for ^{1}H NMR. The relative ratios of these complexes were obtained by integrating their respective pyridine H3 resonances, which are the least affected by the paramagnetic Ru^{III}.

Results

Compound Characterization. The neutral ligand ruthenium(III) complexes exhibit a broad LMCT around 620 nm and intense ligand $\pi \rightarrow \pi^*$ transitions in the ultraviolet. Above pH 7, complexes with guanosine ligands developed an intense band around 415 nm, while the band at 620 nm decreased. The new band at 415 nm is attributed to a $Ru^{II} \rightarrow$ py metal-to-ligand charge transfer (MLCT) transition[13] and is identical to that of [Guo$(NH_3)_4$(py)Ru^{II}]. A second, new band appears at a later time between 700 and 800 nm, depending on the pH, which is in a region where both [$Gua^{2-}(NH_3)_4$(py)Ru^{III}] (788 nm) and *trans*-[(8-$OGuo^-$)(py)$(NH_3)_4Ru^{III}$] (λ_{max} > 776 nm) absorb. ^{1}H NMR spectra of such solutions allowed to react in air confirmed a mixture of both [Gua$(NH_3)_4$(py)Ru^{III}] and *trans*-[(8-OGuo)(py)$(NH_3)_4Ru^{III}$]. In the absence of air, only [Gua$(NH_3)_4$-(py)Ru^{III}] was observed.

The ^{1}H NMR resonances of ruthenium(III) complexes (see experimental section) are quite broadened and shifted by this paramagnetic ion as shown in the spectra in Figure 1. The H3 pyridine proton resonances in [Guo(py)$(NH_3)_4Ru^{III}$] are similar (within 2 ppm) to those in [(py)$(NH_3)_5Ru^{III}$].[14] Assignments of the pyridine H2 and H4 resonances were made on the basis of relative line broadening and by comparison with the spectrum of *trans*-[Isn(Im)$(NH_3)_4Ru^{III}$], which has no H4.[15] In the guanosine complex, δ(H4) is upfield of δ(H2) by 12 ppm, which contrasts with δ(H2) being upfield of δ(H4) by ∼7 ppm in the pentaammine complex.

Significantly narrower NMR peaks between 0 and 10 ppm arise when the pH of the *trans*-pyridine−purine complexes is adjusted into the neutral or basic range. For L = Guo, these sharpened peaks were identical with those of *trans*-[(Guo)(py)-$(NH_3)_4Ru^{II}$]. In addition, a second, similar, but less intense set of narrow resonances, which are also attributed to the guanosine (H8) and pyridine protons was present. These probably arise from ammine ligand loss through base-induced anation. A further indication of this is that, upon oxidation, a new LMCT band grows in at higher energy (λ_{max} = 600 nm), which is consistent with a decrease in charge on the metal center. (Less likely is that these resonances are due to Ru^{IV} complexes, which

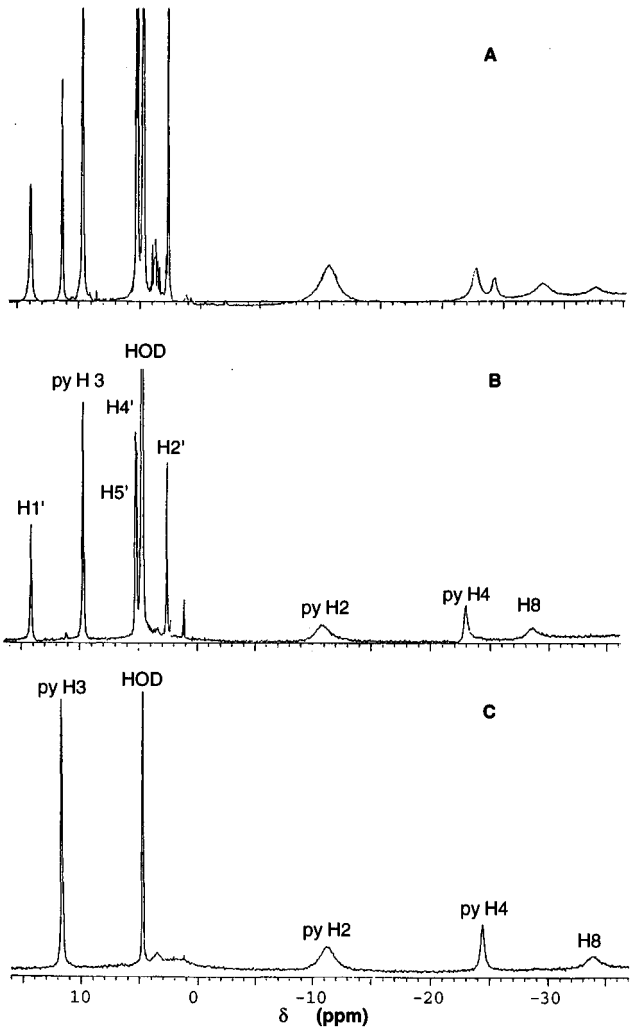

Figure 1. ^{1}H NMR spectra: (a) product mixture of the reaction of *trans*-[(Guo)(py)$(NH_3)_4Ru^{III}$] at pH 12 following removal of the organic, anation, and oxidation products by ion exchange chromatography; (b) *trans*-[(Guo)(py)$(NH_3)_4Ru^{III}$]; (c) *trans*-[(Gua)(py)$(NH_3)_4Ru^{III}$].

are generally paramagnetic.)[16] At pH > 12, the pyridine and guanosine H8 peaks shift slightly due to guanosine ionization at N1 (see pK_a values in experimental section). Sugar resonances were observed at appropriate δ values,[14] except for H5′ signals which may have been obscured by the HOD peak.

Solutions of $[py(NH_3)_5Ru]^{3+}$ disproportionate at pH > 7.[5] ^{1}H NMR spectra of these solutions also revealed two sets of diamagnetic resonances for each pyridine proton. Under the same conditions, but in the presence of ribose, the Ru^{III} was quantitatively converted to Ru^{II} as determined by the absorbance at 407 nm. ^{1}H NMR of the neutral organic material from this reaction, which was obtained by separation on an SP-Sephadex cation exchange column eluted with water, exhibited a resonance (δ = 8.6 ppm) indicative of an aldehydic hydrogen in addition to the ribose resonances in the 3−4 ppm range. This resonance was not present in solutions of *trans*-[(Guo)(py)$(NH_3)_4Ru^{III}$] adjusted to high pH.

Kinetics. The rate of formation of [(Guo)py$(NH_3)_4Ru^{II}$] from the corresponding complex of Ru^{III} was found to be first order in both the ruthenium complex and [OH^-] (Figure 2) and independent of oxygen, yielding the following rate law: $d[Ru^{II}]/dt = k_o[Ru^{III}] + k_1[Ru^{III}][OH^-]$, where $k_o = (2.9 \pm 0.9) \times 10^{-4}$ s^{-1} and $k_1 = 6.4 \pm 0.2$ M^{-1} s^{-1}. Values for k_{obs} are listed in

(12) Sigman, D. S.; Chen, C. B. In *Metal-DNA Interactions*; Tulius, T. D., Ed.; American Chemical Society: Washington, DC, 1989; pp 24−48.
(13) Ford, P.; Rudd, D. F. P.; Gaunder, R.; Taube, H. *J. Am. Chem. Soc.* **1968**, *90*, 1187−94.
(14) Rodriguez-Bailey, V. Ph.D. Thesis, Boston College, Chestnut Hill, MA., 1992.
(15) LaChance-Galang, K. J.; Doan, P. E.; Clarke, M. J.; Rao, U.; Yamano, A.; Hoffman, B. *J. Am. Chem. Soc.* **1995**, *117*, 3529−3538.
(16) Seddon, E. A.; Seddon, K. R. *The Chemistry of Ruthenium*; Elsevier: New York, 1984; pp 1373.

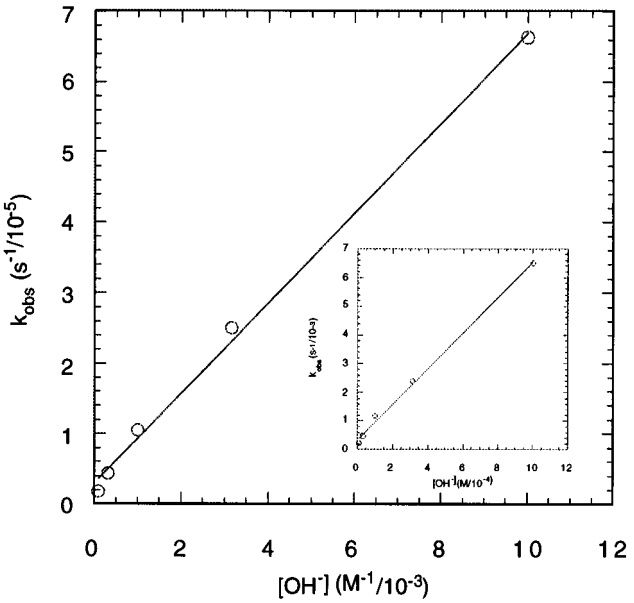

Figure 2. Plot of k_{obs} vs [OH^-] for the disproprotionation of *trans*-[(Guo)(py)$(NH_3)_4Ru^{III}$]. Inset: Plot of log(k) vs pH.

Table 1. Rate Constants for the Disproportionation of *trans*-[L(py)$(NH_3)_4Ru^{III}$] to the Corresponding Ru^{II} and Ru^{IV} Complexes at $T = 25$ °C, $\mu = 0.1$[a]

ligand	k_o ($s^{-1}/10^{-4}$)	k_1 (M^{-1} s^{-1})
9MeGua	0	3.1 ± 0.2
dGuo	3.4 ± 1	6.2 ± 0.2
Guo	2.9 ± 0.9	6.4 ± 0.2
1MeGuo	3.5 ± 1.5	24.7 ± 0.3

[a] Rate law: $d[Ru^{II}]/dt) = k_o[Ru-L] + k_1[Ru-L][OH^-])$.

Table 2. Activation Parameters for k_1 in the Disproportionation of *trans*-[L(py)$(NH_3)_4Ru^{III}$] to the Corresponding Ru^{II} and Ru^{IV} Complexes at $\mu = 0.1$

ligand	$\Delta H^{\ddagger}$ (kcal/mol)	$\Delta S^{\ddagger}$ (cal/(mol K))	pH
Guo	17.4 ± 0.8	2.4 ± 0.1	11.5
dGuo	23 ± 1	21 ± 1	11.0

Supporting Information in Table S-I and the first and second order rate constants for all ligands are summarized in Table 1. At pH 9−10.5, the yield of Ru^{II} was 40−55%, whereas at pH 11−12 the yields were 50−65%. Activation parameters at pH 11.5 are listed in Table 2. Reference to Table 1 shows that ligand modification has a significant effect on the rate such that the 1MeGuo complex disproportionates 4 times faster than the complexes with Guo and dGuo, which ionize at N1 with pK_a values of 7.91 and 8.24, respectively. The second order rate constant for L = Gua was estimated at 1.2×10^{-2} M^{-1} s^{-1} at pH 11.5, which is substantially less than those for all other ligands. At this pH, the guanine ligand is ionized at both N9 and N1, so that the ligand is essentially dianionic. The 100-fold slower rate for the guanine vs the deoxyguanosine complexes allows accurate determinations of the disproportionation and hydrolysis rates for the latter in the presence of contaminants of the former.

Since a solution of [(Guo)py$(NH_3)_4Ru^{III}$] held at pH 9 for 3 half-lives of the disproportionation reaction yielded less than 50% [(Gua)py$(NH_3)_4Ru^{III}$] (see below), the cleavage of the *N*-glycosidic bond takes place following the disproportionation step that produces Ru^{II}. Monitoring the concentration of [(Gua)py$(NH_3)_4Ru^{III}$] spectrophotometrically at 788 nm yielded an absorption curve typical of a sequential reaction in which [(Gua^-)py$(NH_3)_4Ru^{III}$] is formed and is then converted to other products. The observed rate constants for the appearance of the guanine complex are pH-dependent (see Figure S-1 and Table S-II) according to the approximate equation: $k_{obs} = k_o + k_1[OH^-]^{1/2}$. Values for k_o and k_1 are listed in Table 3 with comparison values for other acid-catalyzed rate constants in Table 4. Plots of log(k_{obs}) vs pH for both the Guo and dGuo complexes are linear below pH 12; however, above pH 12 there is a dramatic increase in k_{obs}, suggesting a change in mechanism. Activation parameters for the reaction producing [(Gua)py-$(NH_3)_4Ru^{III}$] via the glycosidic hydrolysis of the Guo and dGuo complexes as determined at pH 11.9 are given in Table 5.

Table 3. Rate Constants for the Appearance of the Corresponding Guanine Complex from the Guanine Nucleoside Complexes of the Listed Ammineruthenium(III) Ions[a]

complex	k_o ($s^{-1}/10^{-5}$)	k_1 ($M^{-1/2}$ $s^{-1}/10^{-3}$)	T (°C)	ref
[Guo(py)$(NH_3)_4Ru^{III}$]	5.5 ± 0.3	$5.3 \pm .6$	25	this work
[dGuo(py)$(NH_3)_4Ru^{III}$]	0.4 ± 0.3	15 ± 5	25	this work
[dGuo$(NH_3)_5Ru^{III}$]	0.54		56	1

[a] Rate law: $d[Ru^{III}Gua]/dt = k_o[Ru-L] + k_1[Ru-L][OH^-]^{1/2})$ at $\mu = 0.1$.

Table 4. Rate Constants for the General-Acid-Catalyzed Hydrolysis of Purine Nucleosides (N−r) or Nucleoside Complexes to Purines (N) or the Corresponding Purine Complex, Respectively[a]

ligand	k_o (s^{-1})	k_1 (M^{-1} s^{-1})	T (°C)	ref
Guo		17.8×10^{-3}	100.6	22
dGuo		6.98×10^{-2}	52.6	22
		3.16×10^{-3}	30.0	
7MeGuo	4.70×10^{-4}	6.03×10^{-2}	100.3	22
[(dGuo)$(NH_3)_5Ru^{III}$]	5.4×10^{-6}		56	1

[a] Rate law: $d[N]/dt = k_o[N-r] + k_1[N-r][H^+])$ at $\mu = 0.1$.

Table 5. Activation Parameters for Reactions Producing [(Gua)(py)$(NH_3)_4Ru^{III}$] from Nucleoside Complexes Compared with Proton Hydrolysis of dGuo

Complex	$\Delta H^{\ddagger}$ (kcal/mol)	$\Delta S^{\ddagger}$ (cal/(mol K))	pH
[(Guo)(py)$(NH_3)_4Ru^{III}$]	24.6 ± 1.6	8.9 ± 0.8	11.9
[(dGuo)(py)$(NH_3)_4Ru^{III}$]	22.1 ± 1.6	4.7 ± 0.5	11.9
H^+dGuo[22]	25 ± 1.0	12.7 ± 2.5	2.31

Product Analysis. ^1H NMR spectra of the noncationic organic material, which was obtained by water elution of the reaction mixture on an ion-exchange column, revealed the major product to be ribose, along with a mixture of other carbohydrate resonances. No purine, amide or aldehydic resonances were observed. Pyridine peaks were occasionally present, when the reaction mixture was oxidized with Ce^{4+} or H_2O_2. There was no evidence of free 8-OGua, which is insoluble at pH < 12, by HPLC or precipitation, nor was free 8-OGuo detected (δ(H1′) ∼ 5.5 ppm).[2,14] Consistent with the presence of ribose, this fraction yielded a positive Bial's test.[10] TLC's of the residue left on evaporation of this fraction yielded a major spot that co-chromatographed with ribose.

A purple to turquoise band eluted next with 0.2 M HCl. UV−visible and NMR spectra indicate that this contained *trans*-[(8-OGuo)(py)$(NH_3)_4Ru^{III}$], *trans*-[(Cl)(py)$(NH_3)_4Ru^{III}$], and other minor, unidentified products, which may be due to ammine loss. A royal blue band eluted next with 0.3 M HCl. ^1H NMR showed this to be a mixture of the starting material, *trans*-[(Guo)(py)$(NH_3)_4Ru^{III}$] and the hydrolyzed product, *trans*-[(Gua)(py)$(NH_3)_4Ru^{III}$], which was identified by comparison with a sample prepared by acid hydrolysis of *trans*-[(dGuo)-(py)$(NH_3)_4Ru^{III}$]. The product distribution at pH < 12, where the hydrolysis reaction is slower, yielded ratios of Ru−Gua: Ru−Guo which decreased from 1:7 at pH 11 to 1:11 at pH 9. A detectable amount of *trans*-[(8-OGuo)(py)$(NH_3)_4Ru^{III}$] was also present, but was negligible in samples taken after three

$t_{1/2}$'s of the disproportionation reaction. At pH > 12 in air, Ru−Gua:Ru−Guo ratios ranged from 1:3 to 1:1, with small amounts of the 8-OGuo complex present. Similar product ratios were obtained at pH 12 with starting material concentrations of 6.15×10^{-5} M and 6.73×10^{-3} M. GC/MS analysis of samples of $[Guo(NH_3)_4(py)Ru^{III}]$ allowed to react in air at pH 10.5 for 2 h yielded ribose and its isomers (arabinose), guanine, and 8-OGua in the proportions of 3:5:1.

When the reaction was performed at pH 12 under an argon atmosphere, the 8-OGuo complex was not detected, and the ratio Ru−Gua:Ru−Guo averaged 1:1. In these reactions, the organic material exhibited a higher yield of ribose, suggesting the other carbohydrate resonances more abundant at lower pH in the presence of O_2 might be due to sugar oxidation products. When complexes with L = Guo and dGuo were subjected to pH 7−10 in air, a peak eventually grew in at 590 nm. Similar spectra were observed when *trans*-$[X(py)(NH_3)_4Ru^{III}]$ (X = Cl^- or SO_4^{2-}) was subjected to the same conditions, so that this peak appears to be due to loss of 8-oxoguanosine following the air oxidation of coordinated guanosine.

Discussion

Structure and Spectra. By analogy to well-characterized complexes of $[L(NH_3)_5Ru^{III}]$ (L = inosine[17] and guanosine[18]), the guanine nucleoside complexes of *trans*-$[(py)(NH_3)_4Ru]$ discussed here are also coordinated at the purine N7. As all the complexes give similar UV−vis and NMR spectra, which are sensitive to the coordination site, the binding site is identical throughout.[14,17] Relative to the analogous pentaammine complexes,[18] the π-acceptor pyridine ligand stabilizes Ru^{II} so that the $E°$'s for the *trans*-pyridine complexes are ~200 mV higher. A combination of decreased σ-donation coupled with a small amount of $d_\pi-\pi$ back-bonding onto the pyridine also shifts the $\pi_{Gua} \rightarrow d_\pi(Ru^{III})$ LMCT bands to lower energy (E_{LMCT}) by 50−60 nm.[18] A similar effect has been observed in a series of *trans*-$[L(Im)(NH_3)_4Ru^{III}]$ complexes, in which E_{LMCT} decreases linearly with the reduction potential for the complex.[15]

In general, the strongly paramagnetically broadened and shifted ^1H NMR resonances (Figure 1) are quite similar (within 2 ppm) to those of the analogous pentaammineruthenium(III) complexes.[14] However, the resonances of the H2′ through H5′ ribose protons in *trans*-$[(Guo)(py)(NH_3)_4Ru^{III}]$ more closely resemble those of $[(Ino)(NH_3)_5Ru^{III}]$ (particularly those for H4′ and H5′ peaks which exhibit coupling). This could arise from a slight decrease in π-electron density on the guanine due to the π-acidity of the pyridine ligand, which would counteract π-donation by the C2-amine so as to weaken hydrogen bonding between the sugar hydroxyls and N3.[19,20] Such an interaction would shift the *syn*−*anti* distribution of the sugar more toward the *anti* component, thereby bringing the guanosine resonances more in line with those of inosine.

Kinetics and Mechanism: Disproportionation. Figure 3 outlines likely pathways for the observed reactions. Since $[(py)(NH_3)_5Ru^{III}]$ disproportionates in basic media,[5] this is likely to be the initiating reaction (Figure 3A) and would be expected to yield approximately 50% Ru^{II} products. That the yield of Ru^{II} can be somewhat higher than this may result from Ru^{IV} oxidation of the sugar. While oxidation of pyridine rings under basic conditions has also been observed to afford Ru^{II} from Ru^{III}

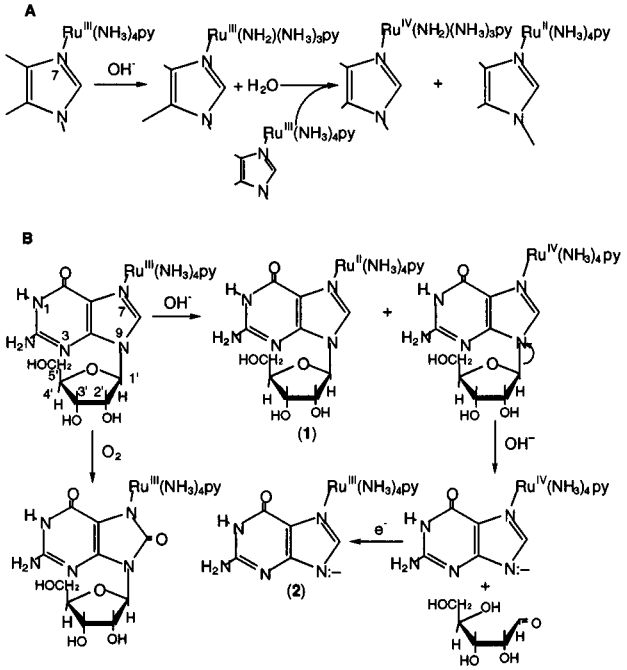

Figure 3. Probable mechanisms: (A) disproportionation of Ru^{III} in *trans*-$[L(py)(NH_3)_4Ru^{III}]$, where L = Guo and dGuo; (B) subsequent *N*-glycosidic bond cleavage. B also shows an oxidative side reaction in the presence of O_2.

pyridyl complexes,[21] no change in the ^1H NMR spectra of the pyridine was observed. Under these conditions, $[py(NH_3)_5Ru^{IV}]$ is strongly oxidizing and may even oxidize hydroxide,[5] so that it is not surprising that there is no direct evidence for Ru^{IV} intermediates. When oxygen is present, some Ru^{II} could also result from autoxidation of the purine, which is thought to proceed through single electron transfer to oxygen with the second electron being transferred internally to Ru^{III}.[2]

Since the appearance of Ru^{II} is first order in $[Ru^{III}]$, even at the lowest complex ion concentrations (6.15×10^{-5} M) employed, the rate-limiting step is not likely to be electron-transfer between ruthenium complexes (Figure 3a), as it is with $[(py)(NH_3)_5Ru^{III}]$.[5] Rather, the first-order hydroxide dependence (Figure 2) suggests that ionization of a coordinated ammine is the rate limiting step (Figure 3a), which may be due to the π-donor properties of the purine imidazole inhibiting proton loss. Further evidence for this is that the slowest disproportionation rate occurs with Gua^{2-}, whose dianionic charge would be the most effective at stabilizing Ru^{III} and suppressing ammine ionization. By the same token, disproportionation is most rapid for the 1MeGuo complex, because this ligand is unable to form an anion. The presence of the relatively large, aromatic purine ligand, which can self-associate and thereby facilitate electron transfer, may also account for the electron transfer's not being rate-limiting.

General Acid *N*-Glycosidic Hydrolysis. Formation of *trans*-$[(Gua)(py)(NH_3)_4Ru^{III}]$ appears to result from a general acid cleavage of the glycosidic bond induced by Ru^{IV} at the N7 position following the disproportionation reaction (Figure 3B). This is in contrast with solutions of *trans*-$[(Ino)(NH_3)_5Ru^{III}]$ held under argon at pH 10.3 for similar periods, which gave no evidence of hydrolysis.[2] As Ru^{IV}Gua is not observed by NMR or UV−vis, only the rate of appearance of Ru^{III}Gua could be monitored. Because the additional step of Ru^{IV} reduction must be included in the mechanistic pathway (Figure 3B), the

(17) Kastner, M. E.; Coffey, K. F.; Clarke, M. J.; Edmonds, S. E.; Eriks, K. *J. Am. Chem. Soc.* **1981**, *103*, 5747−5752.
(18) Clarke, M. J.; Taube, H. *J. Am. Chem. Soc.* **1974**, *96*, 5413−5419.
(19) Haschemeyer, S. E. V.; Sobell, H. M. *Acta. Crystallogr.* **1965**, *19*, 125.
(20) Tavale, S. S.; Sobell, H. M. *J. Mol. Biol.* **1970**, 109−123.
(21) Ghosh, P. K.; Brunschwig, B. S.; Chou, M.; Creutz, C.; Sutin, N. *J. Am. Chem. Soc.* **1984**, *106*, 4772−4783.

gylcosidic hydrolysis rate constants listed in Tables 3 and S2 are probably lower limits.

A number of Lewis acids (proton, methyl group[22] or Ru^{III}; cf. Table 4) coordinated at N7 induce heterolytic cleavage of the *N*-glycosidic bond.[1] In the case of CH_3^+, this yields an oxocarbenium ion on the sugar,[7] which is then hydrated by water or hydroxide. Ru^{III} is the least effective and exhibits an hydrolysis rate 1800 times slower than H^+ and 180 slower than CH_3^+ at 56 °C (estimates made from data in Table 4, pK_a values and activation parameters).[1] Table 5 indicates that $\Delta H^{\ddagger}$ for bond scission by the Ru^{IV} base-assisted pathway is at least 3 kcal less than the proton-assisted pathway. Consequently, the probable net ordering for relative strengths in effecting glycosidic bond cleavage is $Ru^{IV} > H^+ > CH_3^+ > Ru^{III}$. The mechanism postulated in Figure 3b for the general-acid-catalyzed hydrolysis of the *N*-glycosidic bond is analogous to the *N*-glycosidic hydrolytic step in the Maxam−Gilbert guanine-sequencing reaction in which CH_3^+ from $(CH_3)_2SO_4$ induces heterolytic cleavage,[7] so that the reaction reported here appears to be an inorganic analog of this classic DNA cleavage reaction.

Maximum *N*-glycosidic hydrolytic yields occurred at pH 12, with the overall role of hydroxide possibly being complicated by the following: (1) the involvement of at least one redox reaction involving Ru^{IV}, which may decrease the hydrolytic yield at lower pH, (2) the multiple proton ionizations possible on Ru^{III} and Ru^{IV} ammines, and (3) base-catalyzed anation reactions, which decrease the yield at higher pH. One possibility is that Ru^{IV} ammine and imido complexes prefer to react by oxidation, but will react faster by hydrolysis if the sugar is also ionized. In concert with this is the increase in the hydrolytic k_{obs} for free 1MeGuo at pH > 9, where ionization of the sugar may begin to exert a kinetic effect.[22,23] While hydroxide attack at C8 to open the imidazole ring followed by sugar loss to form 2,4,6-triamino-5-foramidopyrimidine[6] is known, no evidence for foramidopyrimidine was found nor was any amide hydrogen detected by NMR.

Acknowledgment. This research was supported by PHS Grant GM26390.

Supporting Information Available: Tables S-1 and S2 containing observed rate constants for disproportionation of $[(Guo)py(NH_3)_4Ru^{III}]$ and observed rate constants for the appearance of *trans*-$[(Gua)py(NH_3)_4Ru^{III}]$ in base from *trans*-$[(L)py(NH_3)_4Ru^{III}]$ and a plot (Figure S-1) of k_{obs} vs $[OH^-]^{1/2}$ for the appearance of *trans*-$[(Gua)py(NH_3)_4Ru^{III}]$ in base from *trans*-$[(Guo)py(NH_3)_4Ru^{III}]$ (inset: plot of $\log(k_{obs})$ vs pH) and Eyring plots (Figure S-2 and S-3) for the disproportionation of *trans*-$[(Guo)(py)(NH_3)_4Ru^{III}]$ and the appearance of *trans*-$[(Gua)py(NH_3)_4Ru^{III}]$ in base from *trans*-$[(Guo)py(NH_3)_4Ru^{III}]$ (3 pages). Ordering information is given on any current masthead page.

IC960798G

(22) Zoltewicz, J. A.; Clark, D. F.; Sharpless, T. W.; Grahe, G. *J. Am. Chem. Soc.* **1970**, *92*, 1741−1750.

(23) Dawson, R. M. C.; Elliott, D. C.; Elliott, W. H.; Jones, K. M. *Data for Biochemical Research*, 2nd ed.; Oxford University Press: Oxford, England, 1969; p 158.